

Direct patterning of micro-features on a polymer substrate using ultrasonic vibration

Young-Soo Seo · Keun Park

Received: 23 November 2011 / Accepted: 27 April 2012 / Published online: 12 May 2012
© Springer-Verlag 2012

Abstract Micro-molding of thermoplastic polymer is a popular fabrication method for micro-devices. Most micro-molding techniques use heated molds to plasticize the thermoplastic polymer, which requires an increased cycle time and additional heating/cooling equipment. In this study, a novel micro-molding process using ultrasonic vibration energy is developed to locally melt the polymer surface by converting the ultrasonic vibration energy into thermal energy, from which the micro-patterns engraved on a sonotrode tip can be rapidly replicated on a polymer substrate. In order to replicate the micro-patterns with high accuracy, the sonotrode should be designed to allow longitudinal vibration only, not transverse or twisting vibrations. In this paper, the sonotrode design was investigated through finite element analyses, from which the resulting natural frequency of the sonotrode can be adjusted to be within the desirable range. Experimental investigations of the ultrasonic patterning were then performed using the sonotrode with the micro-patterns. The effects of various processing parameters on the replication characteristics are also discussed and analyzed statistically in order to find the optimal processing conditions.

1 Introduction

In recent years, the demand for components with micro-features has driven the development of advanced techniques for micro-fabrication of polymer products including

micro-fluidic devices, micro-actuators, and optical components. For example, the increasing requirements to improve the quality of optical products have forced the minimum feature size of the optical components to be reduced to micrometer and nanometer scales (Kang 2004). The micro-molding of thermoplastic polymers is one of the most popular fabrication methods for micro/nano devices because several thousand parts can be produced after a mold insert has been fabricated.

Various molding techniques have been developed to enable the micro-molding of thermoplastic polymers. Among these techniques, hot embossing and micro-injection molding are ranked as the most feasible manufacturing processes (Heckel and Schomburg 2004). The hot embossing process uses a pre-heated mold to imprint micro-patterns on a thermoplastic polymer substrate (Chou and Krauss 1997). Because the micro-structured tool must be heated above the softening temperature of the polymer, this process requires long cycle times to ensure proper cooling and demolding; in general, it requires more than 10 min (Becker and Heim 2000). Recently, rapid mold heating techniques have been used in the hot embossing process; however, these techniques require significant modifications of the embossing tools (Kimerling et al. 2006).

Injection molding is one of the most popular methods in polymer processing due to its high productivity and flexibility, and it has recently been applied to the fabrication of micro-features (Giboz et al. 2007). However, micro-injection molding has difficulty filling the mold due to the frozen layer generated near the mold surface. In order to overcome this difficulty, the mold surfaces should be heated to the softening temperature of the polymer. However, this mold heating increases the cycle time because it must provide sufficient cooling time for appropriate

Y.-S. Seo · K. Park (✉)
Department of Mechanical System Design Engineering,
Seoul National University of Science and Technology,
Seoul 139-743, Republic of Korea
e-mail: kpark@seoultech.ac.kr

demolding. Thus, in order to rapidly heat the mold surfaces without a significant increase in the cycle time, various heating techniques have been developed such as infrared radiation heating (Chang and Hwang 2006), high frequency proximity heating (Yao et al. 2006), and high frequency induction heating (Park and Lee 2010). Although these mold heating techniques are very efficient in the rapid heating of the mold surfaces, they still require additional heating time. Furthermore, these heating techniques require additional heating equipment, which increases the production costs as well as energy consumption.

Recently, ultrasonic waves have been used in the micro-fabrication of thermoplastic polymers in an attempt to provide a more energy efficient solution. Micro-scale ultrasonic welding has been developed for the fabrication of micro-fluidic components (Truckenmüller et al. 2006). In injection molding, the ultrasonic vibration energy was used to improve the microstructures in the weldline regions (Lu et al. 2006) and to plasticize a small amount of polymer for the micro-injection molding (Michaeli et al. 2011). Ultrasonic energy has also been used in hot embossing as an auxiliary heating source for the embossing molds (Liu and Dung 2005; Mekaru et al. 2007). The ultrasonic embossing processes have been further developed to replicate micro-patterns using ultrasonic energy without additional mold heating equipment (Mekaru and Takahashi 2008; Altman et al. 2012). These studies indirectly applied ultrasonic energies in order to sufficiently raise the mold temperature and required additional micro-patterned molds.

In this study, ultrasonic vibration energy is directly applied in order to fabricate micro-features on polymer substrates, not only to raise the mold temperature but to also imprint the micro-patterns on the polymer substrates. For this purpose, the ultrasonic sonotrode was designed to contain the micro-features on its tip, so that its vibration characteristics directly affect the moldability of the micro-patterns. Finite element (FE) analyses were then performed to investigate the vibration characteristics of the sonotrode. Experimental research with statistical analyses was also conducted in order to investigate the effects of the processing parameters on the replication characteristics of the micro-patterns.

2 Configuration of the ultrasonic patterning apparatus

The proposed ultrasonic patterning process aims to locally melt the surface of a polymer substrate, from which the micro-patterns engraved on the sonotrode tip can be directly replicated. The micro-scale vibration of the sonotrode causes repetitive friction between the sonotrode and the thermoplastic polymer. Thus, as a result of friction, the

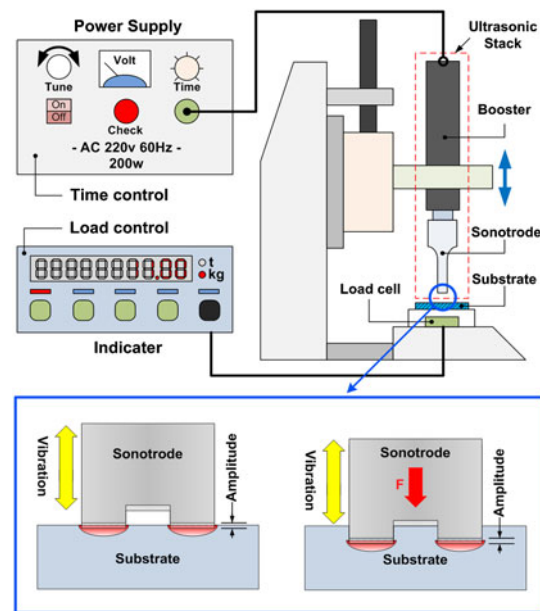


Fig. 1 Configuration of the direct patterning apparatus using ultrasonic vibration

surface region of the polymer substrate is heated repeatedly and is sufficiently softened to be embossed by the pressure of the sonotrode. Figure 1 illustrates the schematic configuration of the ultrasonic patterning apparatus for direct pattern replication. This apparatus consists of a power supply, an ultrasonic stack, and a pressing unit.

As an ultrasonic generator, the power supply delivers a high power AC signal with a frequency of 28 kHz. The ultrasonic stack is composed of a piezoelectric transducer, a booster, and a sonotrode. These three components are tuned to resonate at a specified ultrasonic frequency, from which the sonotrode will resonate under the given ultrasonic excitation. The pressing unit consists of a mechanical press, a mold embedded with a load cell, and a control unit in which various processing parameters can be controlled including the vibration time, embossing depth, and embossing load. This ultrasonic patterning apparatus operates using the following steps: (i) a polymer substrate is installed in the mold, (ii) the sonotrode presses the substrate with ultrasonic excitation, and (iii) the sonotrode recedes and the micro-patterned substrate is ejected.

3 Design and analysis of the ultrasonic sonotrode

3.1 Design of the stepped sonotrode

In this section, the design of a sonotrode is investigated in order to obtain the desired range of resonance frequency. A sonotrode is one of the most important parts of the proposed ultrasonic patterning apparatus because it amplifies

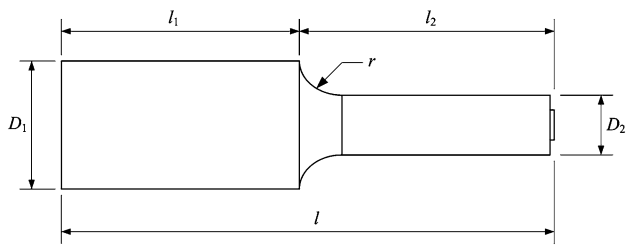


Fig. 2 The shape and dimensional parameters of the stepped sonotrode

the ultrasonic vibration energy from the transducer and transfers the amplified energy to the polymer substrate on which the micro-patterns are replicated. In order to ensure the high energy transmission capability as well as the replication characteristics of the micro-patterns, the vibration characteristics of the sonotrode should be analyzed and optimized.

A sonotrode is usually designed to have an outlet section that is smaller than the inlet section in order to amplify the amount of vibration at its outlet. The most common designs for sonotrode shapes are conical, exponential, and stepped shapes. In this study, the stepped sonotrode was selected due to its high amplification characteristics and manufacturability. Figure 2 shows the shape of the stepped sonotrode with its dimensional parameters.

An important design parameter is the sonotrode length (l) that must be adjusted to be as close as possible to the resonance length. The resonance length of a stepped sonotrode is calculated using the following equation (Seah et al. 1993):

$$l = \frac{1}{2f} \sqrt{\frac{E}{\rho}} \tag{1}$$

where f is the frequency of the ultrasonic wave, and E and ρ are the elastic modulus and density of the sonotrode material, respectively. In this study, AL7075-T651 was used as the sonotrode material, and its elastic modulus and density were 71.7 GPa and 2,810 kg/m³, respectively. The frequency of the ultrasonic wave was 28 kHz, and the resulting length of the sonotrode was determined using Eq. (1).

Assuming that the sonotrode is rotationally symmetric, its dynamic equilibrium equation is given as in Eq. (2) using the one-dimensional wave equation (Amin et al. 1995):

$$\rho A(x) \frac{\partial^2 u(x,t)}{\partial t^2} = E \frac{\partial}{\partial x} \left(A(x) \frac{\partial u(x,t)}{\partial x} \right), \tag{2}$$

where $u(x,t)$ is the amount of vibration in the axial direction and $A(x)$ is the cross-sectional area at the axial position (x). Then, l_1 and l_2 can be determined by solving the differential equation.

Table 1 Specification of the sonotrode with the micro-patterns

Specifications	Value (mm)
Total length (l)	92.5
Shank length (l_1)	45.1
Input diameter (D_1)	28.0
Output diameter (D_2)	13.0
Corner radius (r)	14.0
Amplification magnitude (β)	4.64

The magnitude of amplification (β) for the stepped sonotrode is defined by the ratio of the cross sectional areas, as expressed in Eq. (3). By solving Eqs. (1), (2), and (3), the design parameters for the sonotrode were initially determined as listed in Table 1.

$$\beta = \frac{A_{input}}{A_{output}} = \left(\frac{D_1}{D_2} \right)^2. \tag{3}$$

3.2 FE analyses of the sonotrode with micro-patterns

In Sect. 3.1, the basic design parameters of the sonotrode were determined using analytic calculations. These calculations are based on the assumption that the sonotrode is rotationally symmetric while the sonotrode used in this study includes rotationally asymmetric characteristics such as the micro-patterns on the sonotrode outlet and planar faces in the sonotrode shank. In this study, FE modal analyses were performed to further investigate the vibration characteristics of the sonotrode in a three-dimensional manner.

Figure 3 shows the three-dimensional shape of the sonotrode. In order to remove the effect of element orientation, a uniform mesh structure was constructed using 83,520 hexahedral elements. The frequency range was set between 20 and 35 kHz considering that the excitation frequency was 28 kHz. ANSYSTM was used to perform the FE modal analyses.

Figures 4a through 4d show the basic mode shapes of the sonotrode in the given frequency range. The detailed mode descriptions and the resulting natural frequencies are summarized in Table 2. It can be seen that the first two

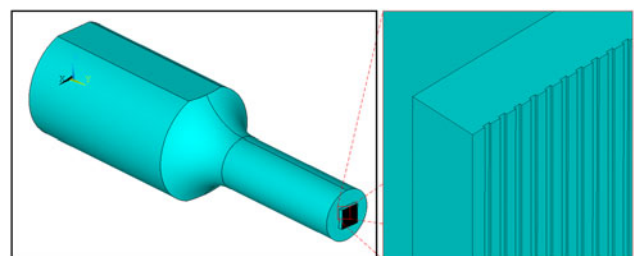


Fig. 3 Three-dimensional model of the sonotrode with micro-patterns

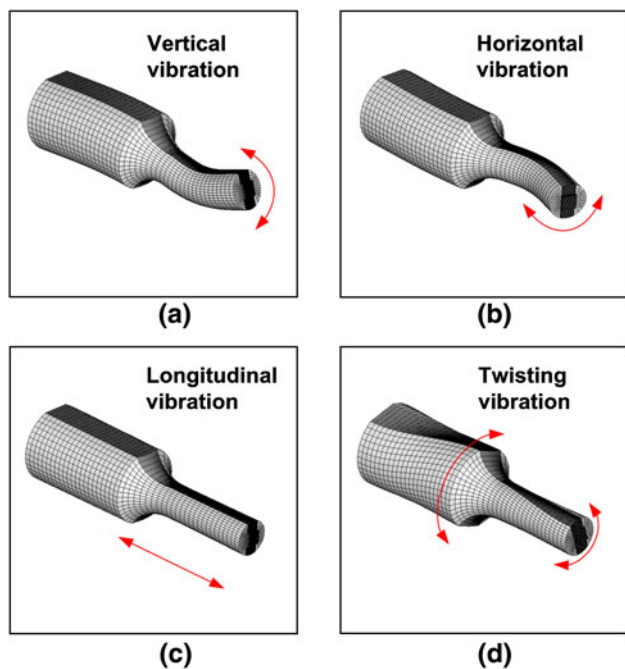


Fig. 4 Vibration mode shapes for the designed sonotrode: **a** mode 1, **b** mode 2, **c** mode 3, and **d** mode 4

Table 2 Results of the FE modal analyses of the sonotrode

Mode	Description	Natural frequency (kHz)
1	Transverse (vertical)	23.520
2	Transverse (horizontal)	23.666
3	Longitudinal	28.608
4	Twisting	32.643

modes correspond to the vertical and horizontal transverse vibration modes. These transverse vibration modes are not appropriate in the proposed ultrasonic patterning system because they weaken the dimensional accuracy of the micro-patterns. The fourth mode is a twisting vibration mode that is also not appropriate. On the contrary, the third mode corresponds to the longitudinal vibration mode, which is the most desirable mode in the proposed system. The natural frequency was 28.608 kHz in this mode, showing a range that is available to resonate with the excitation frequency of the ultrasonic wave.

Figure 5 plots the relative magnitude of the sonotrode vibration in the longitudinal vibration mode. The relative magnitude (γ) was defined by taking the relative value of the deformation at an arbitrary position (x) to the deformation at the inlet, $u(0)$:

$$\gamma(x) = \frac{|u(x)|}{|u(0)|}. \quad (4)$$

The relative magnitude at the output section of the sonotrode ($\gamma(l)$) was calculated to be 4.22. This value

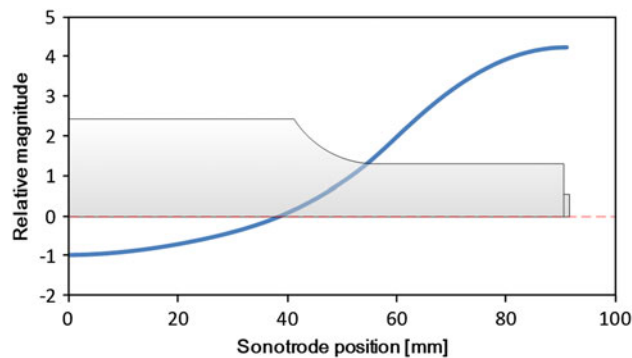


Fig. 5 Relative magnitude of the sonotrode vibration

indicates the amount of amplification of the sonotrode because it was normalized with respect to $u(0)$; that is, the deformation of the input section. Comparing this value with the theoretical estimation of the magnification amplification (4.64), it can be seen that a small amount of deviation (9.1 %) exists due to the three-dimensional features of the sonotrode.

4 Application of ultrasonic energy to micro-pattern replication

4.1 Fabrication of a sonotrode containing micro-patterns

A stepped sonotrode was fabricated reflecting the final design parameters discussed in Sect. 3.2. The natural frequency of the manufactured sonotrode was measured to be 28.663 kHz, which shows a similar value to that of the simulation result. Then, micro-patterns with rectangular shapes were fabricated on the sonotrode tip. Three-axis micro-machining equipment was used to manufacture the micro-patterns. The sonotrode material was AL7075-T6, and fourteen micro-patterns were fabricated on the sonotrode tip. Figure 6 shows a sectional photograph of the micro-patterns with a pitch (P), width (D), and depth (H) of 250, 100, and 33.7 μm , respectively.

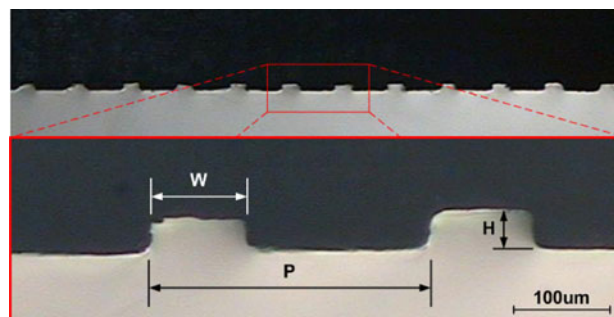


Fig. 6 Micro-patterns on the tip of the sonotrode

4.2 Micro-pattern replication on a polymer substrate

An experiment for ultrasonic patterning was performed using the patterned sonotrode. The workpiece was a poly-methylmethacrylate (PMMA) substrate with a thickness of 500 μm. Three processing parameters, the embossing depth (h), embossing load (f) and vibration time (t), were discussed in terms of the pattern replication characteristics. In order to quantify the embossing depth as a relative measure, the embossing ratio (η) was defined by dividing the embossing depth (h) by the substrate thickness (500 μm).

The ultrasonic patterning experiment was performed using an ultrasonic excitation of 28 kHz. The embossing depth was set to 300 μm, which corresponds to the embossing ratio of 0.6. The embossing load and vibration time were set to 4.0 kgf and 2.5 s, respectively. Figure 7 plots the temperature change on the bottom of the substrate during the embossing process. It can be seen that the maximum temperature of 225.4 °C was obtained after heating for 2.5 s. Considering that the glass transition temperature (T_g) of PMMA is 105 °C, the polymer softening started at 0.81 s and ended at 3.75 s, which corresponds to a softening period of 2.94 s.

Figure 8a is a photograph of the patterned substrate, which demonstrates that the micro-patterns were successfully replicated under the given embossing conditions. In order to investigate the replication characteristics quantitatively, the height of each micro-pattern was measured using a surface profiling apparatus (Rugosurf®90). Figure 8b plots the replicated pattern heights of the fourteen micro-patterns. The mean value of the heights is 27.05 μm, which corresponds to 80.3 % of the replication ratio in height.

4.3 Effects of the processing parameters

In this section, the effects of the processing parameters on the pattern replication characteristics are discussed. Three

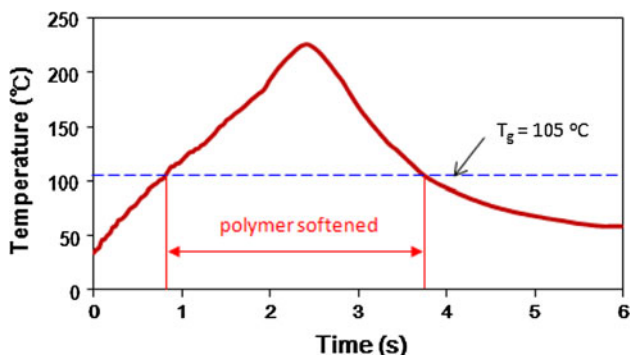
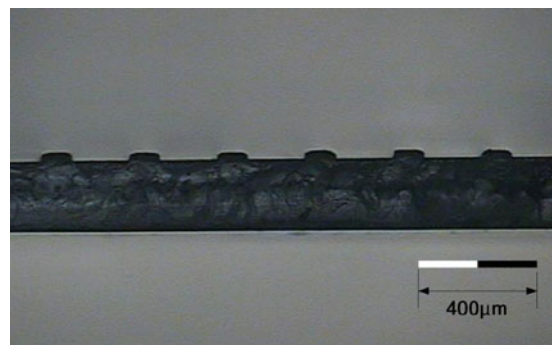
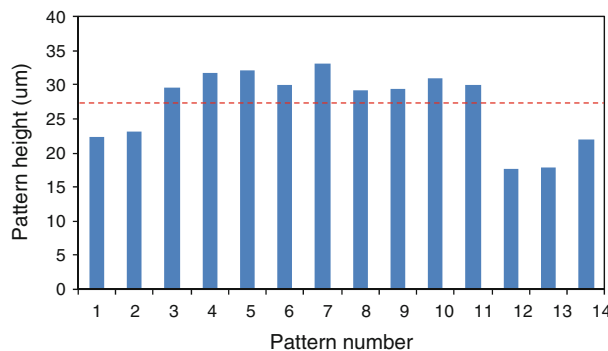


Fig. 7 Temperature change of the substrate during the ultrasonic patterning process



(a)



(b)

Fig. 8 Results of the micro-pattern replication: a sectional image of the patterned substrate and b comparison of replicated pattern heights

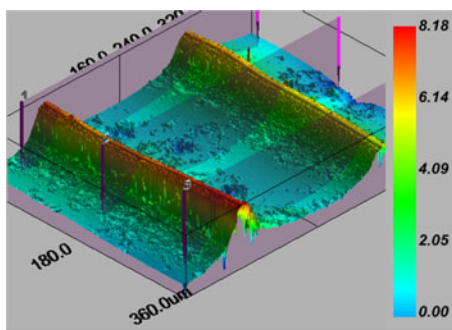
processing parameters, the embossing ratio, embossing load and vibration time, are investigated as separately.

4.3.1 Effects of the embossing ratio

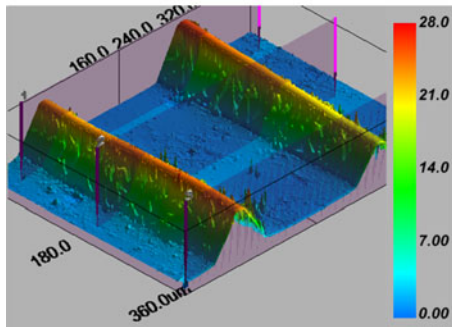
At first, the ultrasonic patterning experiments were performed with an embossing ratio of 0.4–0.8. The embossing load and the vibration time were set at 4.0 kgf and 2.5 s, respectively. Figures 9a through 9c show the measured surface profiles of the micro-patterns for the embossing ratio of 0.4, 0.6, and 0.8. It is demonstrated that the heights of the replicated micro-patterns increased with an increase in the embossing ratio. The detailed results are summarized in Table 3, in which the replication ratio was defined by calculating the relative value of the pattern height to the tool depth. It can be seen that the replication ratio increased to 94.8 % when the embossing ratio was 0.8; that is, 80 % of the original substrate thickness.

4.3.2 Effects of the embossing load

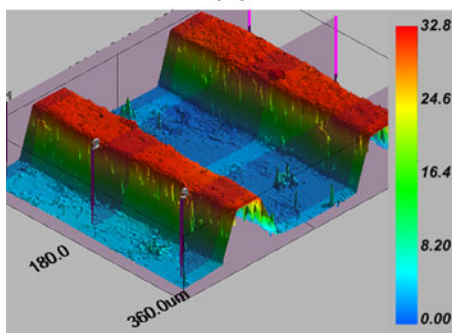
Additional experiments were performed with variations in the embossing load, from 3.0 to 5.0 kgf. In these experiments, the embossing ratio was constant at 0.6. Figures 10a through 10c show the measured surface profiles of the



(a)



(b)



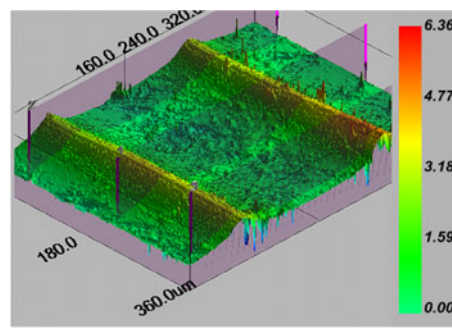
(c)

Fig. 9 Measured surface profiles of the replicated patterns (unit: μm) with variations in the embossing ratio: **a** 0.4, **b** 0.6, and **c** 0.8

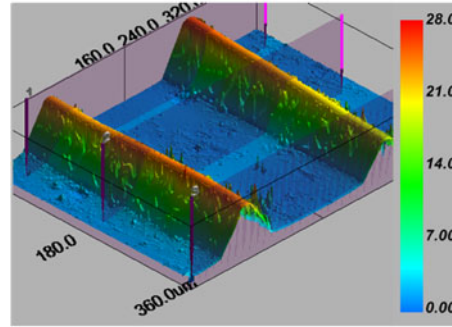
Table 3 Comparison of the pattern heights with variations in the embossing ratio

Embossing ratio	Pattern height (μm)		Replication ratio (%)
	Mean value	Standard deviation	
0.4	7.67	4.94	22.8
0.6	27.05	5.33	80.3
0.8	31.96	2.18	94.8

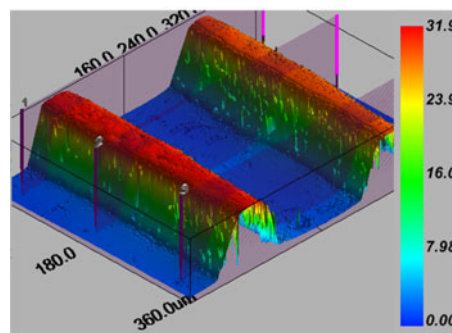
micro-patterns for the embossing loads of 3.0, 4.0, and 5.0 kgf. It can be seen that the increase of the embossing load also improves the replication characteristics of the micro-features. The detailed results are summarized in Table 4, demonstrating that the replication ratio improved to 93.4 % when the embossing load was 5.0 kgf.



(a)



(b)



(c)

Fig. 10 Measured surface profiles of the replicated patterns (unit: μm) with variations in the embossing load: **a** 3 kgf, **b** 4 kgf, and **c** 5 kgf

Table 4 Comparison of the pattern heights with variations in the embossing load

Embossing load (kgf)	Pattern height (μm)		Replication ratio (%)
	Mean value	Standard deviation	
3.0	6.45	5.55	19.1
4.0	27.05	5.33	80.3
5.0	31.46	1.89	93.4

4.3.3 Effects of the vibration time

Further experiments were performed with variations in the vibration time from 1.5 s to 3.5 s. The embossing load and ratio were maintained at 4.0 kgf and 0.6,

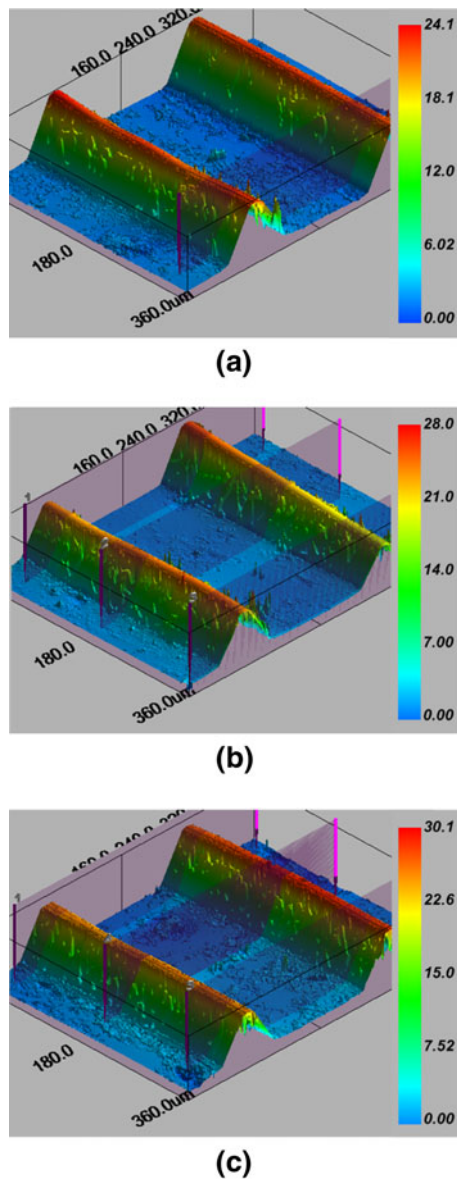


Fig. 11 Measured surface profiles of the replicated patterns (unit: μm) with variations in the vibration time: **a** 1.5 s, **b** 2.5 s, and **c** 3.5 s

respectively. Figures 11a–c show the measured surface profiles of the micro-patterns for the vibration time of 1.5, 2.5, and 3.5 s. The detailed results are summarized in Table 5, demonstrating that the replication ratio varies from 73.1 to 90.1 % as the vibration time increases. Although the increase of the vibration time also improves the replication characteristics, its rate of improvement is less sensitive than those of the previous parameters.

4.4 Design of experiments and statistical analysis

Although the effects of the three processing parameters were investigated in the previous section, their effects were

Table 5 Comparison of the pattern heights with variations in the vibration time

Vibration time (s)	Pattern height (μm)		Replication ratio (%)
	Mean value	Standard deviation	
1.5	24.62	7.05	73.1
2.5	27.05	5.33	80.3
3.5	31.46	4.83	90.1

Table 6 Orthogonal array and the relevant responses of the first DOE

No.	Embossing ratio, η	Embossing load, f (kgf)	Vibration time, λ (s)	Replication ratio, λ (%)
1	0.6	4.0	2.5	80.30
2	0.6	4.0	3.5	90.07
3	0.6	5.0	2.5	93.40
4	0.6	5.0	3.5	90.06
5	0.8	4.0	2.5	94.80
6	0.8	4.0	3.5	90.93
7	0.8	5.0	2.5	94.78
8	0.8	5.0	3.5	91.18

discussed as separately to the experiment design. In this section, the design of experiment (DOE) was applied to systematically investigate the effects of the three parameters considering their mutual interactions. The first screening DOE was performed for the three parameters with two levels as listed in Table 6. Based on the results of the previous section, the level for each parameter was chosen to have a range where the mean value of the replication ratio exceeded 80 %.

A full factorial DOE with two levels (eight experiments) was conducted with six repetitions for each process condition. Figure 12a presents the main effect plots for the replication ratio. It can be seen that the embossing ratio and load exhibit a positive effect on the replication characteristics. In contrast, the vibration time does not demonstrate a significant effect, showing a slightly negative effect. Figure 12b represents the interaction plot between each design parameter. It can be seen that the embossing ratio and load show a strong interaction while the vibration time does not have a significant interaction with the other design parameters. Thus, the vibration time could be removed in the next DOE by fixing it as 2.5 s in order to obtain a more uniform replication.

The second DOE was scheduled using the central composite design (CCD) table in order to apply the response surface method (RSM). Thirteen experiments were scheduled based on the orthogonal array of the two remaining design factors (η and f) as listed in Table 7. The

Fig. 12 DOE results for the replication ratio: **a** the main effect plot and **b** the interaction plot

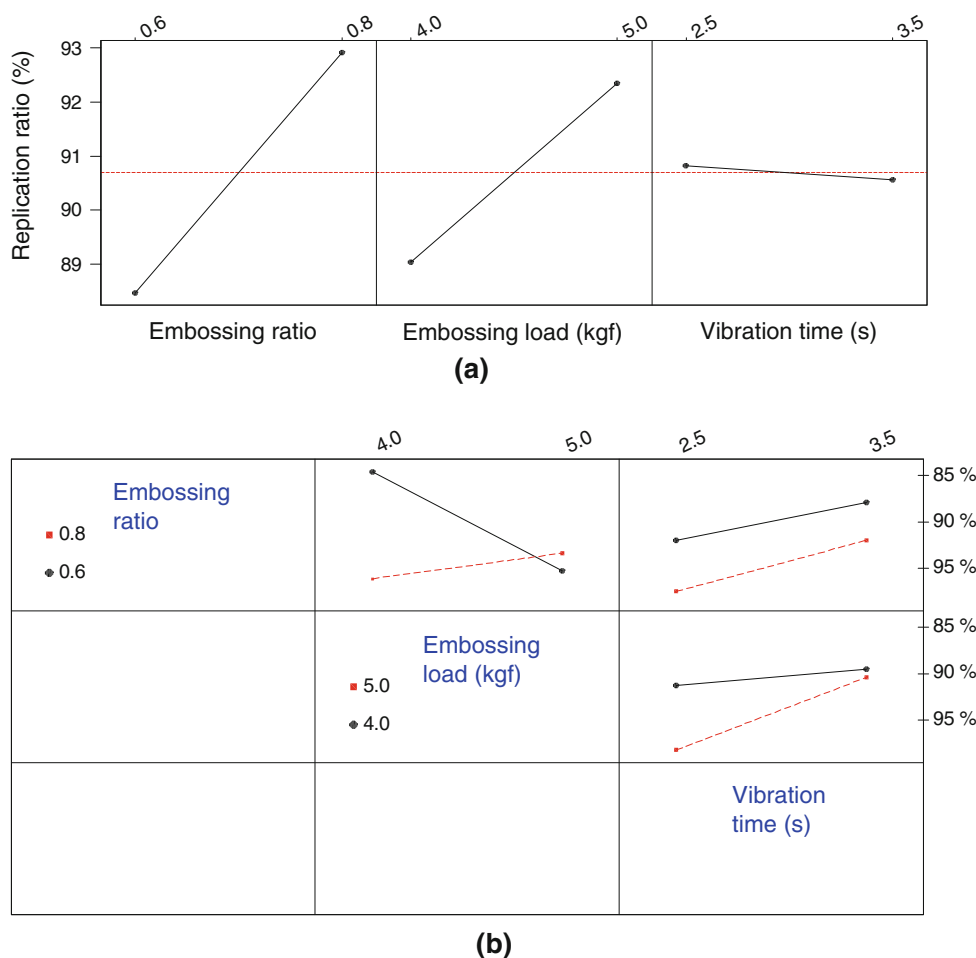


Table 7 Orthogonal array and the relevant responses of the second DOE

No.	Embossing ratio, η	Embossing load, f (kgf)	Replication ratio, λ (%)
1	0.8	5.0	94.78
2	0.8	4.0	94.80
3	0.6	4.0	80.30
4	0.7	3.792	83.85
5	0.7	4.5	88.61
6	0.7	4.5	90.30
7	0.841	4.5	95.50
8	0.7	4.5	89.52
9	0.7	4.5	87.11
10	0.6	5.0	93.40
11	0.7	4.5	87.36
12	0.7	5.207	91.65
13	0.558	4.5	64.12

experiments were conducted based on this schedule with six repetitions, and the resulting responses are also listed in Table 7.

Through the statistical analysis, the quadratic regression model for the response surface of the replication ratio (λ) was obtained as in Eq. (5):

$$\lambda = -217.59 + 738.03\eta + 3.5277f - 262.50\eta^2 - 65.60\eta f + 5.380f^2, \tag{5}$$

where η and f are the embossing ratio and load, respectively. The optimal processing parameters can then be found based on this regression model. The maximum embossing ratio was restrained to 0.8 in order to avoid the case that the remaining thickness becomes too small, i.e. <100 μm .

The optimal embossing load to maximize the replication ratio was then obtained as 6.08 kgf. Further experiments were conducted under this optimized condition, and the resulting replication ratio was improved to 95.4 %. Figure 13 plots the resulting pattern heights of fourteen micro-patterns, demonstrating that the replication characteristics are remarkably improved for all patterns when compared with Fig. 8b.

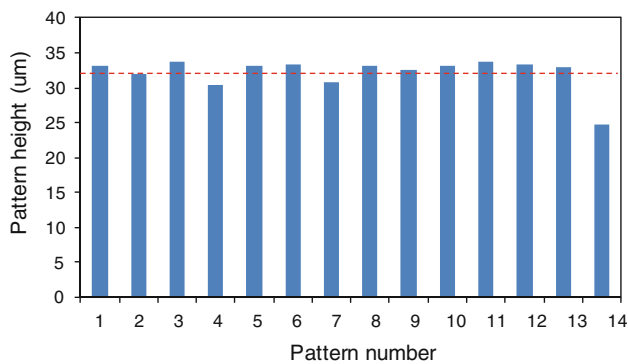


Fig. 13 Comparison of pattern heights replicated under the optimal conditions

5 Conclusion

In this study, a micro-patterning process on a plastic substrate using ultrasonic energy was proposed. This ultrasonic patterning process aims to locally melt the surface of a polymer substrate, from which the micro-patterns engraved on the sonotrode tip can be directly replicated. FE modal analyses were performed in order to investigate the vibration characteristics of the sonotrode. Through the FE analyses, the design parameters of the sonotrode were determined in order to obtain the resonance conditions for the longitudinal vibration under an excitation frequency of 28 kHz. A number of micro-patterns were fabricated on the sonotrode tip that was used to replicate the micro-patterns on the polymer substrate. Experiments were then performed with variations of the embossing ratio, embossing load, and vibration time. Statistical analyses were performed combining the two-step DOE and RSM to find the optimal processing conditions, from which 95.4 % replication ratio was obtained.

Considering the proposed process requires less than 5 s per cycle, it is expected that the process will be able to replace the conventional injection molding and hot embossing processes. Based on these results, future research is expected to implement this process in the manufacturing of high quality micro/nano components.

Acknowledgments This research was financially supported through the Basic Science Research Program of the National Research Foundation (NRF) funded by the Ministry of Education, Science and Technology (Grant number: 2010-0008435). The authors would like to thank Dr. Yoon of the Korea Institute of Industrial Technology (KITECH) for his support on the micro-machining of the sonotrode pattern.

References

- Altman B, Ahren R, Welle A, Dingreiter H, Schneider M, Schober A (2012) Microstructuring of multiwall plates for three-dimensional cell culture applications by ultrasonic embossing. *Biomed Microdevices* 14:291–301
- Amin SG, Ahmed MHW, Youssef HA (1995) Computer-aided design of acoustic horns for ultrasonic machining using finite-element analysis. *J Mater Process Technol* 55:254–260
- Becker H, Heim U (2000) Hot embossing as a method for the fabrication of polymer high aspect ratio structures. *Sensors Actuators* 83:130–135
- Chang PC, Hwang SJ (2006) Experimental investigation of infrared rapid surface heating for injection molding. *J Appl Polym Sci* 102:3704–3713
- Chou SY, Krauss PR (1997) Imprint lithography with sub-10 nm feature size and high throughput microelectronics engineering. *Microelectron Eng* 35:237–240
- Giboz J, Copponnex T, Méle P (2007) Microinjection molding of thermoplastic polymers: a review. *J Micromech Microeng* 17:R96–R109
- Heckel M, Schomburg WK (2004) Review on micro molding of thermoplastic polymers. *J Micromech Microeng* 14:R1–R14
- Kang S (2004) Replication technology for micro-nano optical components. *Jap J Appl Phys* 43:5706–5716
- Kimerling TE, Liu W, Kim BH, Yao D (2006) Rapid hot embossing of polymer microfeatures. *Microsyst Technol* 12:730–735
- Liu SJ, Dung YT (2005) Hot embossing precise structure onto plastic plates by ultrasonic vibration. *Polym Eng Sci* 45:915–925
- Lu C, Yu X, Guo S (2006) The mechanism of ultrasonic improvement of weld line strength of injection molded polystyrene and polystyrene/polyethylene blend parts. *J Polym Sci Part B Polym Phys* 44:1520–1530
- Mekaru H, Takahashi M (2008) Ultrasonic nanoimprint on poly(ethylene terephthalate) at room temperature. *Jpn J Appl Phys* 47:5178–5184
- Mekaru H, Goto H, Takahashi M (2007) Development of ultrasonic micro hot embossing technology. *Microelectron Eng* 84:1282–1287
- Michaeli W, Kamps T, Hopmann C (2011) Manufacturing of polymer micro parts by ultrasonic plasticization and direct injection. *Microsyst Technol* 17:243–249
- Park K, Lee SI (2010) Localized mold heating with the aid of selective induction for injection molding of high aspect ratio microfeatures. *J Micromech Microeng* 20:035002
- Seah KHW, Wong YS, Lee LC (1993) Design of tool holders for ultrasonic machining using FEM. *J Mater Process Technol* 37:801–816
- Truckenmüller R, Cheng Y, Ahrens R, Bahrs H, Fischer G, Lehmann J (2006) Micro ultrasonic welding: joining of chemically inert polymer microparts for single material fluidic components and systems. *Microsyst Technol* 12:1027–1029
- Yao D, Kimerling TE, Kim B (2006) High-frequency proximity heating for injection molding applications. *Polym Eng Sci* 46:938–945